Supporting Information

Mechanistic Insight into the Z-E Isomerization Catalysis of Azobenzenes Mediated by Bare and Core-Shell Gold Nanoparticles

Sabrina Simoncelli[a-c] and Pedro F. Aramendía*[a,b]

[a] Centro de Investigaciones en Bionanociencias "Elizabeth Jares-Erijman"(CIBION-CONICET) Godoy Cruz 2390, 1425 Buenos Aires, Argentina. [b] Departamento de Química Inorgánica, Analítica y Química Física, Facultad de Ciencias Exactas y Naturales, Universidad de Buenos Aires, Pabellón 2. Ciudad Universitaria. 1428 Buenos Aires, Argentina.[c] Instituto de Química Física de Materiales, Ambiente y Energía, (INQUIMAE-CONICET). Pabellón 2. Ciudad Universitaria. 1428 Buenos Aires, Argentina.

E-mail: pedro.aramendia@cibion.conicet.gov.ar

Table of Contents

List of Figures and Tables

S1: Nanoparticle characterization

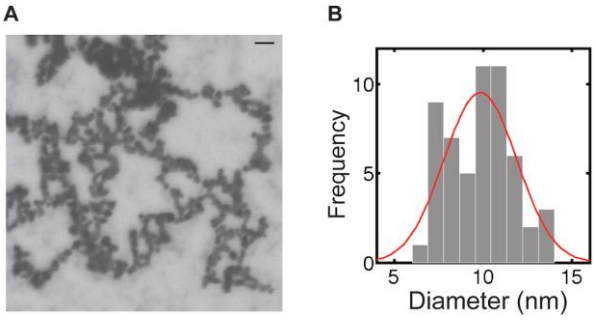

Figure S1. SEM micrograph (A) and diameter histogram (B) of 'semi-naked' photochemically synthesized AuNPs of 10 ± 2 nm diameter. Scale bar represents 20 nm. Histogram was constructed with sample set size $n > 50$.

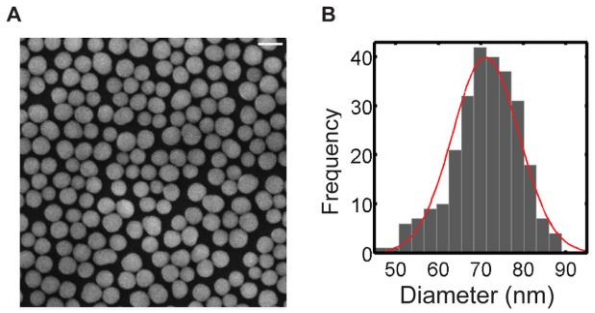

Figure S2. SEM micrograph (A) and diameter histogram (B) of silica nanoparticles. of 71 ± 8 nm diameter. Scale bar represents 100 nm. Histogram was constructed with sample set size $n > 100$.

S2: Influence of AuNPs on the Z-E isomerization rate of NO_2-DAB, DABCYL and NO_2-HAB

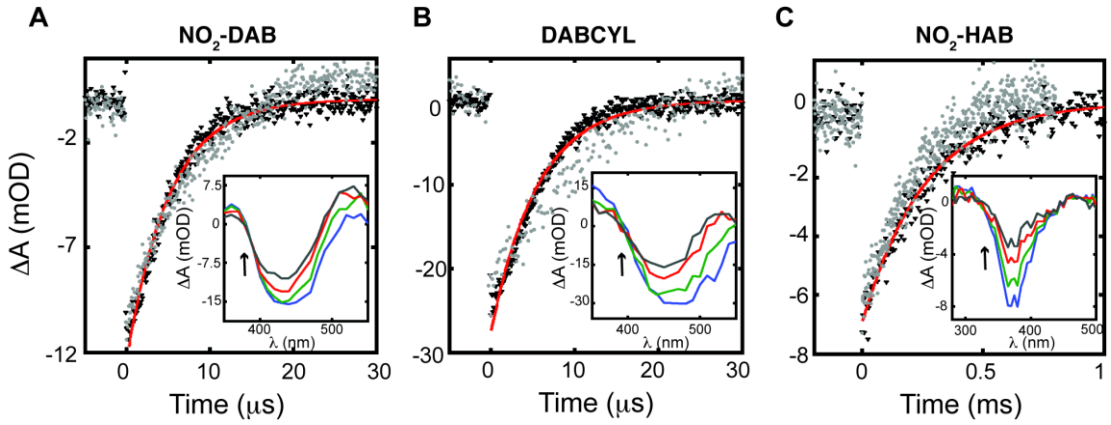

Figure S3. Transient absorbance difference at 430, 430, and 370 nm, respectively, for a 15 μM solution of (A) NO_2-DAB; (B) DABCYL and (C) NO_2-HAB measured immediately after pulsed laser excitation at 460, 460, and 355 nm (3.5 mJ, 6 ns), respectively, in acetonitrile (ACN) (grey circles) and in 200 pM 'semi-naked' AuNPs suspensions (black triangles). The temporal scale for the free dye in solution was contracted 1000 times for the NO_2-DAB and DABCYL; and 50 times for the NO_2-HAB. The red line corresponds to the monoexponential fit of the experimental data. The insets correspond to the difference absorption spectra of each system at different time after the excitation pulse.

S3: Influence of pH on the Z-E isomerization kinetic rate of azobenzenes/AuNPs systems

The pH of the AuNPs synthesized following the Turkevich[1] method is determined by the relative concentration of trisodium citrate and $HAuCl_4$. $HAuCl_4$ is a strong acid that completely dissociates in water into $AuCl_4^-$ and H^+. The Cl^- - OH^- equilibrium substitution modifies the acidity of the medium according to the following reaction,

$$AuCl_x(OH)_{4-x}^- + 2H_2O \rightleftharpoons AuCl_{x-1}(OH)_{5-x}^- + H_3O^+ + Cl^-$$

The equilibrium constants associated with the substitution of 1, 2, 3 or 4 chloride ions by hydroxyl are pK_1 = 5.7, pK_2 = 6.5, pK_3 = 7.6, pK_4 = 8.6, respectively.[2] On the other hand, trisodium citrate is a weak acid (pK_a's: 3.2, 4.8 and 6.4) and its addition to

$HAuCl_4$ solution provokes increase of the pH. Turkevich synthesis requires 0.25 mM $HAuCl_4$ with an 8 to 1 trisodium citrate:$HAuCl_4$ ratio. Consequently the trisodium citrate will dominate the pH of the AuNPs solution, which is close to pH = 6.

In a recent publication the group of Scaiano reported that photochemically synthetized 'semi-naked' AuNPs also present a catalytic effect over the E-Z isomerization reaction of some substituted AB.[3] These NPs are obtained by the reduction of $HAuCl_4$ to Au^0 by superoxide radicals produced from H_2O_2. H_2O_2 is a base (pK_a = 11.4) that acts as a strong oxidant in acidic medium.[4] The synthesis is performed by UVA irradiation of 0.33 mM $HAuCl_4$ and 0.01 mM H_2O_2 solution. The pH is therefore dominated by the $HAuCl_4$ concentration, being close to pH = 3. The pH control experiments were then performed with this 'semi-naked' AuNPs as their pH is lower than the pH of the Turkevich AuNPs. Therefore, if no acceleration is observed when matching the pH to that of the more acidic NPs, no effect is expected for the less acidic Turkevich ones.

Specifically the acidity control experiments where performed by preparing 3 mL acetonitrile or MiliQ water solutions of 50 μM of the corresponding azobenzenes or 15 μM for the NO_2-DAB, DABCYL, and NO_2-HAB probes to which 100 μL of 6 nM 'semi-naked' AuNPs or 100 μL of a 1.32 mM HCl and 0.01 mM H_2O_2 solution was added. The concentration of the HCl solution was chosen to ensure 4 equivalents of protons with respect to the Au^{+3} equivalents used in the NPs synthesis.

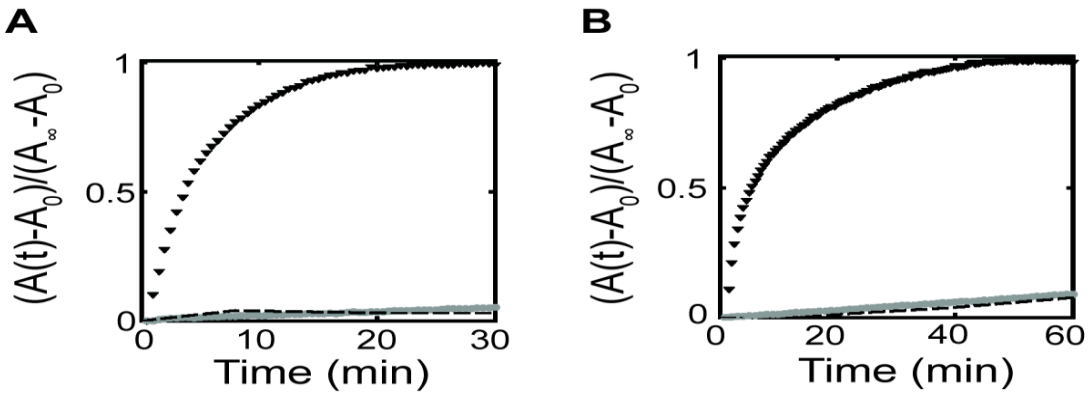

Figure S4. Growth of the E isomer measured at 320 nm and 360 nm, respectively, for 50 μM (A) AB in water and (B) DEO-AB in ACN:water (5:1) in the presence of 200 pM 'semi-naked' AuNPs (black triangles) or 44 μM HCl (grey circles) immediately after the photolysis flash. The dashed black line near the abscissa axis represents the temporal growth of the E isomer in the absence of AuNPs.

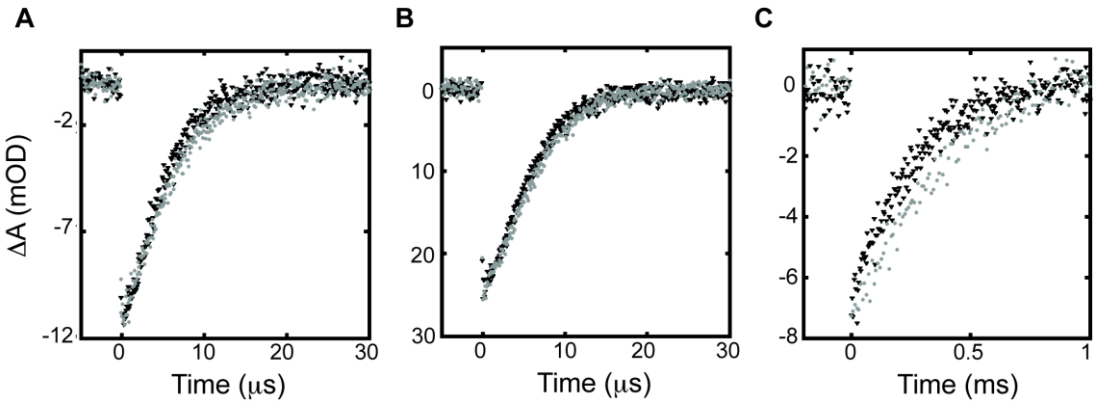

Figure S5. Transient absorbance difference at 430, 430, and 370 nm, respectively, for a 15 μM solution of (A) NO_2-DAB; (B) DABCYL and (C) NO_2-HAB measured immediately after pulsed laser excitation at 460, 460, and 355 nm (3.5 mJ, 6 ns), respectively, in the presence of 200 pM 'semi-naked' AuNPs (black triangles) or 44 μM of HCl (grey circles) in ACN.

S4: Influence of AB and AuNPs concentration on the Z-E isomerization rate of azobenzenes /AuNPs systems

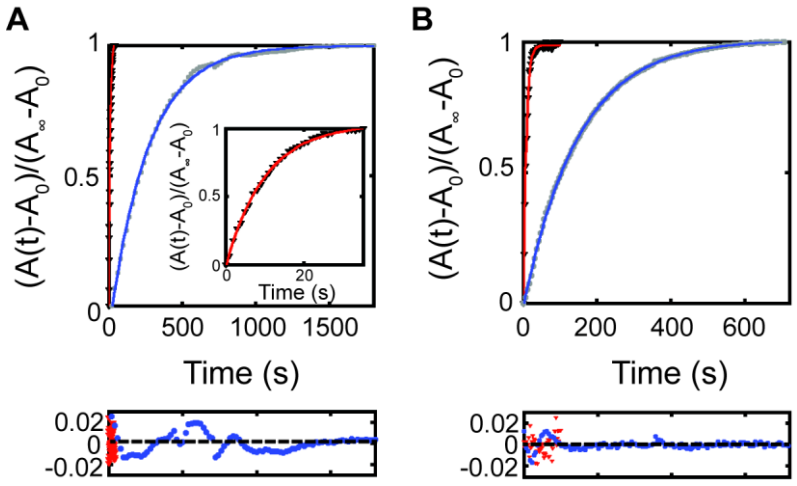

Figure S6. Growth of the E-AB isomer measured at 320 nm for aqueous solutions of (A) 50 μM AB and 200 pM (grey circles) or 1 nM (black triangles) AuNPs, and (B) 300 pM AuNPs and 9 μM (black triangles) or 50 μM (grey circles) AB. The red and blue lines correspond to the monoexponential fit of the experimental data. The inset displays the temporal amplification (A). The bottom figures display the residuals of the monoexponential fits.

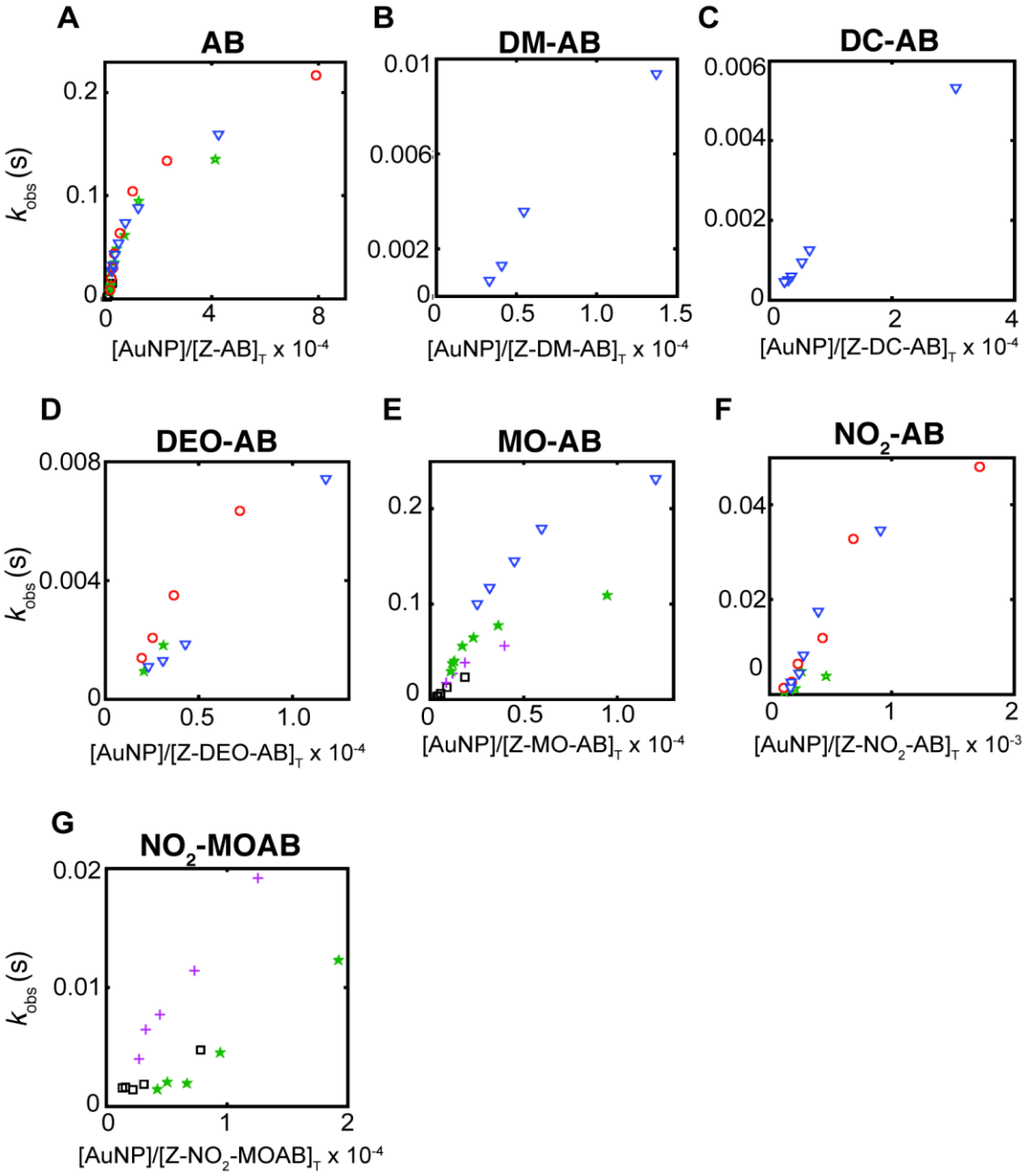

Figure S7. Thermal Z-E isomerization reaction rate constant as a function of the [(Z-AB)$_T$]/[AuNP] for aqueous solutions (A and E) or ACN:water solutions (B-D and F-G) of azobenzenes and AuNPs. The different symbols correspond to [AuNP] of □: 100 pM; +: 200 pM; ⋆: 300 pM; ○: 400 pM and□∇: 500 pM.

S5: Z-E isomerization in gold-silica core-shell nanoparticles (AuNPs@SiO$_2$)

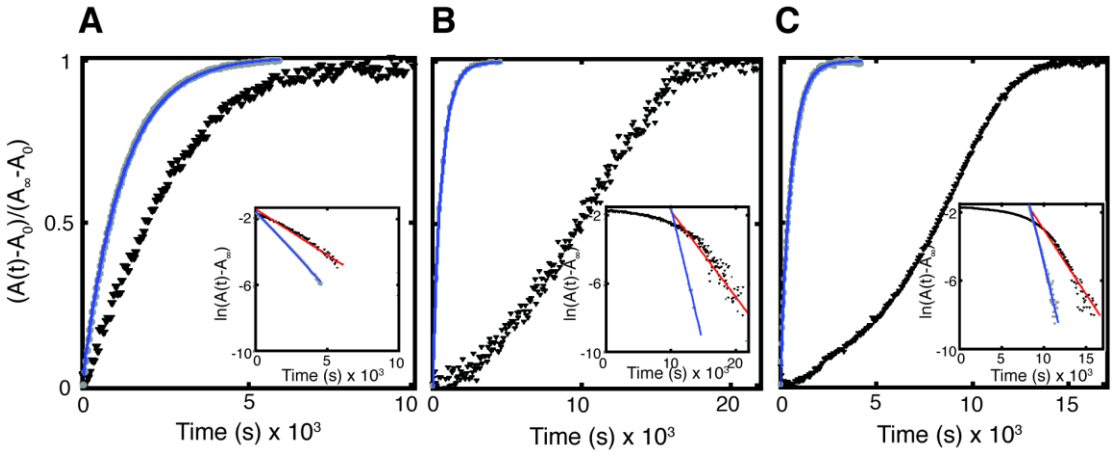

Figure S8. Growth of the E-AB isomer measured at 320 nm for ethanolic solutions of 8 μM AB in suspension of AuNPs@SiO_2 of various silica shell thickness: (A) 4 ± 1 nm ([AuNP] = 1.0 nM); (B) 7 ± 1 nm ([AuNP] = 1.0 nM) and (C) 13 ± 1 nm ([AuNP] = 0.6 nM) immediately after (black triangles) or after 12 hs (grey circles) NPs addition to the AB solution. The blue lines represent the best monoexponential fit of the data. The insets correspond to the logarithmic representation of the absorbance growth. The data recorded immediately after NPs addition were temporally delayed for a better comparison. The blue and red lines correspond to the best linear fits.

S6: Determination of the first order thermal isomerization rate associated to the AuNPs.

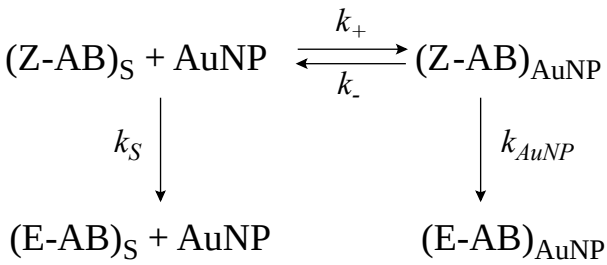

Scheme S1. Mechanism for the microheterogeneous dark Z-E isomerization catalyzed by AuNPs.

The observed first order reaction rate constant for the thermal Z-E isomerization is a global rate constant, k_{obs}, that contains the information of the isomerization rate constants in solution, k_S, and in the vicinity of AuNPs, k_{AuNP}. Considering the rigorous definition of k_{obs} and the mass balance for the *Z*-AB isomer,

$$k_{obs} = -\frac{1}{[Z-AB]_T} \cdot \frac{d[Z-AB]_T}{dt} \qquad \text{(eq. S1)}$$

$$[Z-AB]_T = [Z-AB]_S + [Z-AB]_{AuNP} \quad \text{(eq. S2)}$$

one obtains that k_{obs} is a weighted average of k_S and k_{AuNP} (eq. S3),

$$k_{obs} = \frac{[Z-AB]_S}{[Z-AB]_T} \cdot \left(-\frac{1}{[Z-AB]_S} \cdot \frac{d[Z-AB]_S}{dt} \right) + \frac{[Z-AB]_{AuNP}}{[Z-AB]_T} \cdot \left(-\frac{1}{[Z-AB]_{AuNP}} \cdot \frac{d[Z-AB]_{AuNP}}{dt} \right)$$

$$= k_S \cdot f_S + k_{AuNP} \cdot f_{AuNP} \quad \text{(eq. S3)}$$

where f_S and f_{AuNP} corresponds to the fraction of molecules associated to the solution and disperse phase, respectively. Temporal variations in $[Z\text{-}AB]_S$ and $[Z\text{-}AB]_{AuNP}$ can be expressed considering the kinetic microheterogeneous mechanism of Scheme S1 (eq. S4 and S5).

$$\frac{d[Z-AB]_S}{dt} = -(k_S + k_+ \cdot [AuNP])[Z-AB]_S + k_- \cdot [Z-AB]_{AuNP} \quad \text{(eq. S4)}$$

$$\frac{d[Z-AB]_{AuNP}}{dt} = k_+ \cdot [Z-AB]_S \cdot [AuNP] - (k_{AuNP} + k_-)[Z-AB]_{AuNP} \quad \text{(eq. S5)}$$

The matrix formulation of these differential kinetic equations (eq. S6) is well characterized by a kinetic scheme with two well-separated relaxation times: a fast time, τ_{fast}, that is not observed, and a slow time, τ_{slow}, that relates to $1/k_{obs}$.

$$\begin{pmatrix} -(k_S + k_+ \cdot [AuNP]) & k_- \\ k_+ \cdot [AuNP] & (k_- + k_{AuNP}) \end{pmatrix} \quad \text{(eq. S6)}$$

Assuming rapid equilibration for the reactant exchange step compared to the isomerization rate constants, $k_+[AuNP]$; $k_- >> k_S$; k_{AuNP}, it follows that,

$$\frac{1}{\tau_{fast}} = k_+ \cdot [AuNP] + k_- \quad \text{(eq. S7)}$$

$$\frac{1}{\tau_{slow}} = \frac{(k_S + k_+ \cdot [AuNP]) \cdot (k_{AuNP} + k_-) - k_+ \cdot k_- \cdot [AuNP]}{k_+ \cdot [AuNP] + k_-} \quad \text{(eq. S8)}$$

and particularly,

$$k_{obs} = \frac{1}{\tau_{slow}} = \frac{k_+ \cdot [AuNP]}{k_+ \cdot [AuNP] + k_-} \cdot k_{AuNP} + \frac{k_-}{k_+ \cdot [AuNP] + k_-} \cdot k_S \quad \text{(eq. S9)}$$

which equals eq. S3. Equation S9 allows us to interpret that the molar fraction of Z-AB molecules associated to each phase directly depends on the adsorption-desorption AB-AuNP equilibrium. Specifically, f_S and f_{AuNP} can be calculated assuming that the $[Z\text{-}AB]_{AuNP}$ can be expressed as a function of average number of catalytic sites associated to a single AuNP, $\langle n \rangle$, such that the mass balance of eq. S2 is express as eq. S10.

$$[Z-AB]_T = [Z-AB]_S + \langle n \rangle \cdot [AuNP] \quad \text{(eq. S10)}$$

Eq. S10 considers that the volume of the continuous phase can be approximated to the total volume of the system. This assumption, is valid, as the total volume fraction occupied by the AuNPs is less than 2 x 10^{-6}, as calculated using eq. S11,

$$f = v_{AuNP} [AuNP] \cdot N_A \quad \text{(eq. S11)}$$

where N_A is the Avogadro's number and v_{AuNP} the volume of a single AuNP.

S7: Estimation of the maximum number of adsorption sites per AuNP

The number of total adsorption sites per AuNP can be estimated considering different approaches. Gold is a metal that crystallizes with *fcc* structure. The polycrystalline surface of gold is mainly dominated by the (111), (100) and (110) crystallographic orientations. In particular, spherical AuNPs can be approximated as a truncated octahedron bounded by {111} and {100} planes whit higher contribution of the Au(111) surface.[5] Particularly spherical AuNPs have been synthesized having up to 97% of Au(111) surface contribution.[6] Therefore, as a first approximation, we can assume that AuNPs can be well represented as a Au(111) surface. In this regard, the group of Crommie has been studying since 2005 the intramolecular structure and self assembly behavior of AB and substituted azobenzenes over the Au(111) surface.[7–10] They found that azobenzene molecules create a variety of surface structures whose

commensurability with the surface periodicity depends on the molecular coverage.[10] The proposed geometry of Figure S9-A allow to estimate as 1.83 nm^2 the surface covered by one azobenzene molecule, assuming a 60° angle between the major and minor side of the parallelogram.[10] Further, considering the 0.5 nm distance separation between parallel azobenzenes chains, the maximum number of binding sites per spherical AuNP of 15 nm diameter is ~ 1.1 x 10^3.

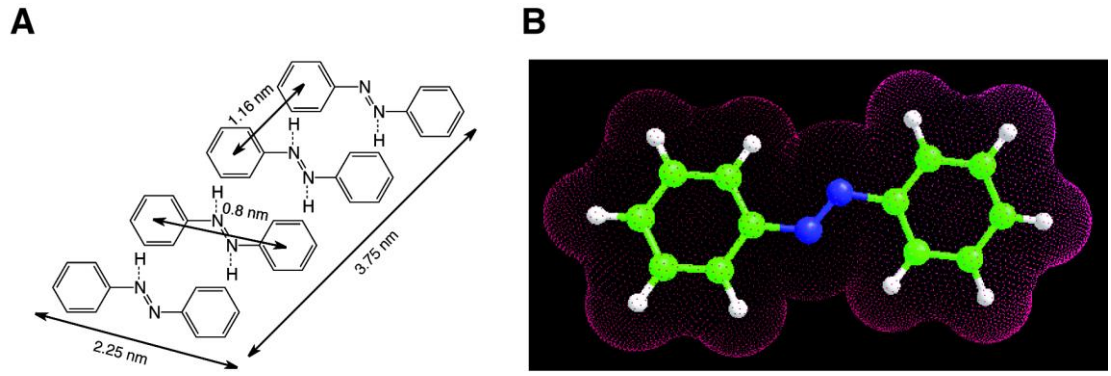

Figure S9. (A) Proposed geometry of azobenzene molecules over Au(111) surface taken from reference 10. (B) Graphic representation (pink dots) of the van der Waals surface determined with the grid method for AB. The white, green and blue sphere represent the hydrogen, carbon and nitrogen atoms, respectively.

A different way to estimate the total number of azobenzene molecules bound per AuNP consists in approximating the surface of each azobenzene compound by molecular modeling methods. Surface calculation optimization of the molecular geometry was performed with the Polak Ribière algorithm in HyperChem 8.0. The molecular energy was minimized with AMBER force field. van der Waals molecular surface was determined using the QSAR plug-in (Figure S9-B) finding values between 1.93 nm^2 for AB up to 2.77 nm^2 for DEO-AB. Finally, assuming a monolayer coverage of AB over the AuNPs, the number of catalytic sites in a spherical 15 nm diameter AuNP is estimated between ~ 1.5 x 10^3 to 1.0 x 10^3. This estimation is similar to the one obtained considering the experimental STM geometrical parameters of AB over the Au(111). In view of these results, we decided to approximated n_{max} as ~ 10^3 binding sites per AuNP independently of the nature of the azobenzene substituents.

S8: Derivation of the diffusion equation

Fick's equation for steady state radial diffusion (eq. S1) has the following general solution (eq. S13),[11]

$$\frac{d}{dr}\left(r^2 \frac{d[Z-AB(r)]}{dr} \right) = 0 \qquad \text{(eq. S12)}$$

$$[Z-AB(r)] = B + A/r \qquad \text{(eq. S13)}$$

where A and B are constants to be determined by the boundary conditions eq. S14 and eq. S15.

$$[Z-AB(r_{NP})] = 0 \qquad \text{(eq. S14)}$$

$$[Z-AB(r_{NP}+h_{SiO2})] = [Z-AB] \qquad \text{(eq. S15)}$$

The first boundary condition states that the concentration of Z-AB is zero over the metallic surface. This is related to immediate Z-E isomerization reaction over the AuNP with respect to the measurements timescale. The second boundary condition considers that Z-AB concentration over the silica surface equals the Z-AB concentration in solution. Further, the latter can be approximated to the average Z-AB concentration, as the fraction of volume occupied by the AuNPs is negligible compared to the total volume. Steady state Z-AB concentration profile depends then on the AuNP radius, r_{NP}, and the silica layer thickness, h_{SiO2}, according to eq. S16.

$$[Z-AB(r)] = [Z-AB] \cdot \frac{r_{NP}+h_{SiO2}}{h_{SiO2}} \cdot \frac{r-r_{NP}}{r} \qquad \text{(eq. S16)}$$

Equation S16 allows us to express the flux of Z-AB molecules trough the silica layer of one AuNP@SiO_2 as,

$$\frac{dn}{dt} = 4\pi \cdot D_{AB-SiO2} \cdot [Z-AB] \cdot \frac{r_{NP} \cdot (r_{NP}+h_{SiO2})}{h_{SiO2}} \qquad \text{(eq. S17)}$$

This expression states that the only pathway associated to the decrease of Z-AB concentration in the solution is related to the flux of molecules passing trough the silica layer that isomerize on the metallic surface. Finally taking into account all the AuNP@SiO_2 of the reaction media we obtain the following expressions,

$$\frac{d[Z-AB]}{dt} = -[Z-AB]\cdot 4\pi\cdot[AuNP]\cdot N_A\cdot D_{AB-SiO2}\cdot\frac{r_{NP}\cdot(r_{NP}+h_{SiO2})}{h_{SiO2}} \quad \text{(eq. S18)}$$

$$[Z-AB]_T = [Z-AB]_T^{t=t_0}\cdot e^{-4\pi\cdot[AuNP]\cdot N_A\cdot D_{AB-SiO2}\cdot\frac{r_{NP}\cdot(r_{NP}+h_{SiO2})}{h_{SiO2}}\cdot t} \quad \text{(eq. S19)}$$

from which we can derive the diffusion coefficient of AB molecules in silica, $D_{AB\text{-}SiO2}$, from the fit of the first order rate constant of the diffusion controlled process, k_{diff}, as

$$D_{AB-SiO2} = \frac{k_{diff}}{4\pi\cdot[AuNP]\cdot N_A}\cdot\frac{h_{SiO2}}{r_{NP}(r_{NP}+h_{SiO2})} \quad \text{(eq. S20)}$$

S9: References

1. J. Turkevich, P. C. Stevenson, and J. Hillier, *Discuss. Faraday Soc.*, 1951, **11**, 55–75.

2. D. V. Goia and E. Matijević, *Colloids Surfaces A Physicochem. Eng. Asp.*, 1999, **146**, 139–152.

3. G. L. Hallett-Tapley, C. D'Alfonso, N. L. Pacioni, C. D. McTiernan, M. González-Béjar, O. Lanzalunga, E. I. Alarcon, and J. C. Scaiano, *Chem. Commun.*, 2013, **49**, 10073–5.

4. K. L. McGilvray, J. Granger, M. Correia, J. T. Banks, and J. C. Scaiano, *Phys. Chem. Chem. Phys.*, 2011, **13**, 11914–11918.

5. A. R. Tao, S. Habas, and P. Yang, *Small*, 2008, **4**, 310–325.

6. M. R. Rahman, F. S. Saleh, T. Okajima, and T. Ohsaka, *Langmuir*, 2011, **27**, 5126–35.

7. J. Cho, L. Berbil-Bautista, N. Levy, D. Poulsen, J. M. J. Fréchet, and M. F. Crommie, *J. Chem. Phys.*, 2010, **133**, 234707.

8. N. Levy, M. J. Comstock, J. Cho, L. Berbil-bautista, A. Kirakosian, F. Lauterwasser, D. A. Poulsen, J. M. J. Fre, M. F. Crommie, M. Sciences, V. Di, and L. Berkeley, *Nano Lett.*, 2009, **9**, 935–939.

9. M. J. Comstock, N. Levy, J. Cho, L. Berbil-Bautista, M. F. Crommie, D. a. Poulsen, and J. M. J. Fréchet, *Appl. Phys. Lett.*, 2008, **92**, 123107.

10. A. Kirakosian, M. Comstock, J. Cho, and M. Crommie, *Phys. Rev. B*, 2005, **71**, 113409.

11. J. Crank, in *Mathematics of Diffusion*, Clarendon Press, Oxford, Second., 1975, pp. 11–27.